"This is the peer reviewed version of the following article: [J Phycol, 2018]. which has been published in final form at [https://onlinelibrary.wiley.com/doi/abs/10.1111/jpy.12759]. This article may be used for non-commercial purposes in accordance with Wiley Terms and Conditions for Self-Archiving."

DR. KIRRALEE BAKER (Orcid ID: 0000-0003-3008-2513)

Article type : Regular Article

Thermal niche evolution of functional traits in a tropical marine phototroph¹

Kirralee G. Baker³

C3- Climate Change Cluster, University of Technology Sydney, Sydney, 2007, New South Wales, Australia

Dale T Radford

C3- Climate Change Cluster, University of Technology Sydney, Sydney, 2007, New South Wales, Australia

Christian Evenhuis

C3- Climate Change Cluster, University of Technology Sydney, Sydney, 2007, New South Wales, Australia

Unnikrishnan Kuzhiumparam

C3- Climate Change Cluster, University of Technology Sydney, Sydney, 2007, New South Wales, Australia

Peter J. Ralph

C3- Climate Change Cluster, University of Technology Sydney, Sydney, 2007, New South Wales, Australia

This article has been accepted for publication and undergone full peer review but has not been through the copyediting, typesetting, pagination and proofreading process, which may lead to differences between this version and the Version of Record. Please cite this article as doi: 10.1111/jpy.12759

Martina.Doblin@uts.edu.au

+61 2 95148307

C3- Climate Change Cluster, University of Technology Sydney, Sydney, 2007, New South Wales, Australia

³Current address:

School of Biological Sciences, University of Essex, Wivenhoe Park, Colchester, CO4 3SQ, Essex, United Kingdom

Running title: Costs and benefits of high-temperature adaptation

Editorial Responsibility: M. Wood (Associate Editor)

ABSTRACT

Land-based plants and ocean-dwelling microbial phototrophs known as phytoplankton, are together responsible for almost all global primary production. Habitat warming associated with anthropogenic climate change has detrimentally impacted marine primary production, with the effects observed on regional and global scales. In contrast to slower-growing higher plants, there is considerable potential for phytoplankton to evolve rapidly with changing environmental conditions. The energetic constraints associated with adaptation in phytoplankton are not yet understood, but are central to forecasting how global biogeochemical cycles respond to contemporary ocean change. Here, we demonstrate a number of potential

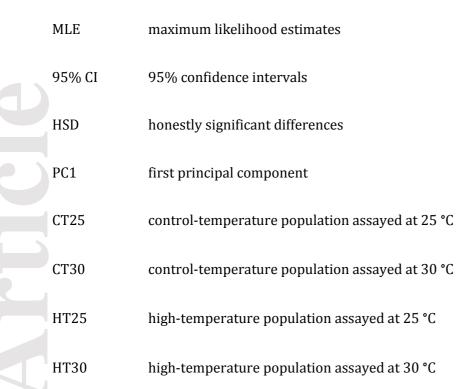
trade-offs associated with high-temperature adaptation in a tropical microbial eukaryote, *Amphidinium massartii* (dinoflagellate). Most notably, the population became high-temperature specialized (higher fitness within a narrower thermal envelope and higher thermal optimum), and had a greater nutrient requirement for carbon, nitrogen and phosphorus. Evidently, the energetic constraints associated with living at elevated temperature alter competiveness along other environmental gradients. While high-temperature adaptation led to an irreversible change in biochemical composition (i.e., an increase in fatty acid saturation), the mechanisms underpinning thermal evolution in phytoplankton remain unclear, and will be crucial to understanding whether the trade-offs observed here are species-specific or are representative of the evolutionary constraints in all phytoplankton.

Key index words: adaptation, phytoplankton, thermal performance curves, global warming, thermal niche.

ABBREVIATIONS

SST	sea surface temperatures
TPCs	thermal performance curve(s)
НТ	high temperature
СТ	control temperature
CT _{min}	critical minimum temperature
CT _{max}	critical maximum temperature
T_{opt}	Thermal optimum/optima

	LEDs	light emitting diodes
	GPP	gross primary productivity
	Lex_{50}	Time point at which 50% of the population was viable
	РАМ	pulse amplitude modulated
	LCs	fluorescence light curves
	PFD	photon flux densities
	F'	minimum fluorescence under actinic illumination
	F _M '	maximum fluorescence under actinic illumination
	$\Phi_{ ext{PSII}}$	effective quantum yield
	rETR	relative electron transport rate
	P-I	photosynthesis-irradiance
U	α	light utilization efficiency
	E _k	light saturation coefficient
	Chl	Chlorophyll
	FA	fatty acid
	FAME	fatty-acid methyl ester
	GC	gas chromatography
	GC-MS	gas chromatography- mass spectrometry
	U/S ratio	unsaturation to saturation ratio
	V _{max}	maximum trait value



INTRODUCTION

Of all abiotic factors that regulate life on Earth, temperature is crucially important because of its universal effects on enzymatic, biochemical and metabolic processes that control nearly all physiological functions (Johnston and Bennett 1996). A recent resurgence in thermal biology research has been prompted by global climate change, particularly in the marine environment, where warming sea surface temperatures (SST) have been linked to reduced ocean productivity (Behrenfeld et al. 2006). Central to these thermally-driven changes are marine phytoplankton, a diverse range of photosynthetic microbes that are responsible for nearly half of global primary productivity and whose metabolic activity mediates most of the global biogeochemical cycles (N, P, trace metals; Falkowski et al. 1998). Despite temperature being a fundamental regulator of phytoplankton metabolic activity, physiology and ecology (Raven and Geider 1988, Davison 1991, Kulk et al. 2012, Thomas et al. 2012), our understanding of how phytoplankton respond to supra-optimal temperatures, especially over long (evolutionary) time scales is limited.

Life thrives within a tolerable range of temperatures, defined as the thermal niche, and outside this range conditions become inhibitory or lethal (Huey and Stevenson 1979, Huey and Kingsolver 1989). Natural populations of phytoplankton have the potential to encounter 'stressful' temperatures, and their survival is dependent upon their ability to adjust to spatial and temporal environmental changes that occur on overlapping timescales. Within an individuals' lifetime (i.e., hours-days), phytoplankton respond by adjusting their physiology, a process known as acclimatization, in order to better suit their natural surroundings (Geider et al. 1997, Flynn 2001). The degree to which organisms are able to acclimatize is determined by their phenotypic plasticity, the ability of an individual to alter certain characteristics or traits. Comparatively, when thermal regimes change and persist on inter-generational timescales (i.e., weeks to years), such as those currently faced by phytoplankton inhabiting the surface layers of the contemporary ocean (rise in long-term mean by approximately +2°C by 2100; IPCC 2014), the survival of a species is ultimately governed by its capacity for adaptation (Hoffmann and Sgro 2011), i.e., genetic changes (via alterations in DNA sequence) and standing genetic variation (Reusch and Boyd 2013). Most studies on the effects of warming on ocean phytoplankton have been of short duration (days-weeks; Robison and Warner 2006, Claquin et al. 2008, Feng et al. 2008, Fu et al. 2008) and therefore have examined acclimatization, or acclimation as it known when studied under artificial conditions in the laboratory. Very few experiments have examined responses in the long term, a major uncertainty in forecasts of future ocean primary productivity.

Experimental evolution studies on bacteria have provided much insight into capacity for adaptation to supra-optimal temperatures (Lenski and Bennett 1993, Elena and Lenski 2003, Bennett and Lenski 2007) but these types of experiments have only recently been considered in the context of phytoplankton and climate change (Collins and Bell 2004, Reusch and Boyd 2013). Many of the long-term (>500 generation) experiments with phytoplankton have focused on the impacts of ocean acidification, reviewed by Collins et al. (2014) and studies of thermal adaptation have generally been restricted to quantifying the effects on fitness (i.e., growth rate;

Huertas et al. 2011, Schluter et al. 2014, Listmann et al. 2016). However, an important factor determining high-temperature evolution, is the adaptability of functional traits, as these are the underlying elements of a phenotype that mediate growth, reproduction, survival and ecological function (Litchman and Klausmeier 2008). For example, the biochemical adaptation of membranes (e.g., changes in fatty acid saturation) may be an important mechanism for coping with high-temperature conditions in both algae and higher plants (Tchernov et al. 2004, Boyd et al. 2010, Zhu et al. 2018).

The adaptation of functional traits ultimately imposes energetic costs to the organism, and is often expressed as trade-offs (inverse relationships) between a range of functional traits (Angilletta 2013). For phytoplankton, the trade-offs of high-temperature adaptation are not yet known but are likely to have profound implications for the metabolism and ecology of marine ecosystems because many functional traits (e.g., cell size and nutrient uptake) are directly or indirectly related to ecological and biogeochemical processes (Falkowski et al. 1998, Litchman and Klausmeier 2008).

To understand the ecological and biogeochemical implications of living at high temperatures, we assessed the potential shift in functional traits (approximately 500 generations of exposure) at supra-optimal temperature (ambient +5°C) in a free-living, widely-distributed tropical dinoflagellate, *Amphidinium massartii*. Specifically, we hypothesized that adaptation to supraoptimal temperature would manifest itself as an alteration in the shape and/or position of the thermal performance curve (TPCs) for one or more key phytoplankton traits (growth, carbon fixation and net flux of dissolved nutrients) in the high-temperature (HT) population, and that some traits would potentially be non-reversible in reciprocal transplant assays. Consequently, for the first time in a dinoflagellate species, we examine the adaptability of the thermal niche of fitness and other key functional traits (specific growth rate, cell volume, unsaturation ratio of

fatty acids, chlorophyll *a* content, maximum electron transport rate, and saturating irradiance) and assess how long term exposure to high temperature in an individual species has the capacity to alter an organisms' thermal plasticity.

MATERIALS AND METHODS

Strain and long-term culture establishment

The tropical benthic dinoflagellate, *Amphidinium massartii* CS-259 was obtained from the Australian National Algae Culture Collection (CSIRO, Hobart, Australia). This strain (CS-259) was originally isolated in 1987 from Kurrimine Beach, Queensland, Australia and taxonomically verified as *A. massartii* using nuclear (ITS, LSU rRNA) and mitochondrial (cytochrome b) gene markers, as well as light and scanning electron microscopy (Murray et al. 2012). According to LSU rRNA (929 bp), strain CS-259 is genetically distinct (differing by ~8%) from other known strains of *A. massartii* (Murray et al. 2012). Members of the *Amphidinium* genus are considered 'model dinoflagellates' for both genetic and ecological studies due to their relatively small genome size (when compared to other dinoflagellates) and genetic transformability for use in DNA manipulation studies (Lohuis and Miller 1998, LaJeunesse et al. 2005), abundance and wide distribution in benthic systems (Lee et al. 2003) and relatively rapid reproductive rates that make them easy to culture.

We established a single selection cell line (n = 1) of a high-temperature population (HTpopulation) of *A. massartii* by transferring the parent culture from the culture collection conditions of 25°C through a series of increasing temperatures (+2°C steps) until a sub-lethal temperature (for this species, 30°C) was reached (Hou 2011), a process known as ratchet culturing (Reboud et al. 2007). Both the parent and the ratcheted population were maintained at their respective temperatures (25°C and 30°C) in semi-continuous batch culture for more than three years (~500 generations) to establish the control-temperature (CT-population) and HT-population respectively. Cultures were acclimated to an irradiance of 100 µmol photons · m⁻

² · s⁻¹ on a 12 h:12 h light:dark cycle in seawater medium (0.2 μm filtered coastal seawater obtained from the Port Hacking National Reference Station, PH100, New South Wales, Australia; www.imos.org.au) with modified f/2 enrichment (lacking silicic acid; Guillard and Ryther 1962) before experimentation commenced.

Our experimental approach was comprised of two separate designs. The first experiment involved a thermal gradient block where small volume cultures (40 mL) were assayed across a wide range of temperatures to examine thermal niche evolution of fitness (specific growth rate), primary production, and nutrient uptake. In the second experiment, larger volume cultures (250 mL) were used in a reciprocal transplant assay (examined under control (25°C) and hightemperature (30°C) conditions) to test whether individual traits (specific growth rate, cell volume, unsaturation ratio of fatty acids, chlorophyll *a* content, maximum electron transport rate, and saturating irradiance) are plastic or become irreversible following adaptation to high temperature. In both experiments, similar sampling regimes were adopted whereby cultures were sampled daily and traits were measured in exponential growth phase. In the following sections we first define how each trait was measured and then go on to describe each of the experimental designs in detail.

Characterisation of phenotype: trait analysis

To quantify traits in the CT- and HT-populations, cultures (40 mL) were grown in triplicate glass vessels for at least five generations over a comprehensive range of temperatures ($\sim 2^{\circ}$ C intervals between 17 and 40°C) in an effort to span the critical temperatures (CT_{min} and CT_{max}) for each trait. Irradiance (100 µmol photons \cdot m⁻² \cdot s⁻¹ on a 12 h:12 h, light: dark cycle) was provided from above by an array of LEDs (Schenzen Cidly Group, China). One mL samples were harvested daily to measure growth, cell viability, photophysiology and dissolved inorganic nutrient stocks. Each replicate was monitored independently (using daily cell count measurements) in order to target exponential phase, when subsamples for gross primary productivity (GPP) assays were harvested.

Phenotype fitness. Growth rate and cell viability was assessed using a mortality assay in combination with flow cytometry, as described in Baker et al. (2016). In order to discriminate between dead and living cells, samples were harvested and incubated in the presence of a nucleic acid stain (SYTOX green, Molecular Probes, Leiden, The Netherlands; final concentration 0.5 μ M). Growth and mortality rate estimates were then made using the abundance of viable and non-viable cells, respectively. Fitness (i.e., specific growth rates) was calculated by fitting a linear regression to the natural logarithm values of each biological replicate during exponential growth phase. At temperatures at which growth ceased, a lethal exposure time (i.e., the time at which 50% of the population was viable; Lex₅₀) was calculated for each population. Mortality data in both treatments were first adjusted for the observed mortality at the T_{opt} and the data were then fitted with an exposure-response function for computation of Lex₅₀.

Carbon Assimilation. To estimate the gross primary productivity (GPP) of exponentially growing cells across the temperature gradient, photosynthetic carbon fixation rates were measured using ¹⁴C-labelled bicarbonate in small volume incubations as described in Baker et al. (2016). Briefly, radiolabeled NaH¹⁴CO₃ (stock solution 1.85×10^7 Bq) was added to 5 mL of culture in clear glass tubes (1.5μ Ci per tube) and incubated in the thermal gradient block for 60–80 min under the growth irradiance. Incubations were terminated by transferring the contents of each tube to a scintillation jar that was acidified with 100 µL 6 M HCl and shaken on an orbital shaker for 12 h to remove inorganic ¹⁴C. Scintillation fluid ($10 \text{ mL Ultima Gold}^{TM}$; Perkin Elmer) was then added to each sample, vigorously shaken and left for 3 h before counting. Counting time was set to 5 min so that counts were within a 5% counting error.

Photophysiology. To test for adaptation of key photophysiological parameters, we used pulse amplitude modulated (PAM) fluorometry to obtain steady-state fluorescence light curves (LCs) using a Water-PAM (Walz GmbH, Effeltrich, Germany). Samples were dark-adapted for 15 min before each LC was started. The photon flux densities (PFD) used for all LCs were supplied as red light (650 nm) in increasing intensities of 0, 1, 11, 21, 36, 56, 81, 111 and 146 µmol photons • m⁻² • s⁻¹. Each PFD step was run for 4 min with a saturating pulse every 30 sec to obtain the minimum and maximum fluorescence under actinic illumination (F' and F_M' , respectively). The average of the last three measurements of F' and F_M' for each PFD was used to calculate the effective quantum yield (Φ_{PSII}) which is equal to ($F_M' - F'$)/ F_M' , and in turn the relative electron transport rate (rETR) calculated as the PFD × Φ_{PSII} (Ralph and Gademann (2005). Finally, a photosynthesis-irradiance (P-I) curve was then modeled by fitting rETR to a Jassby-Platt model (Jassby and Platt 1976) to derive the light utilization efficiency (α) and the light saturation coefficient (E_k) according to the equations in Ralph and Gademann (2005).

Elemental uptake of nitrogen and phosphorus. To estimate net cellular uptake of N and P (added to cultures as NO₃⁻ and PO₄³⁻), subsamples (1 mL) were harvested daily and centrifuged at 5000*g* (5 min at 20°C). Supernatant volumes (500 μL) were removed and stored frozen at -20°C until colorimetric analysis of N and P was conducted (within 3 months) using the methods of Schnetger and Lehners (2014) and Hoenig et al. (1989), respectively, as described in Baker et al. (2016). Net flux was calculated as the difference between nutrient concentrations normalised to cell abundance at the start and end of the exponential phase.

Cell size. Cells were harvested in exponential growth phase when volumes of 2 mL were sampled, fixed in glutaraldehyde (final concentration 1% v/v) and stored at 4°C until later analysis. Samples were loaded into a Sedgewick-Rafter counting chamber (Graticules Limited, England) and images captured via microscopy (×200; bright field; Nikon Eclipse Ti, Nikon, Japan) that were analysed via an image processing script written for Image-J software as described in Suggett et al. (2015). Cell volume was estimated from cell diameter assuming cells were ellipsoidal (Hillebrand et al. 1999). A minimum of 1500 cells was measured and the cell volume was estimated as the median of the population.

Chlorophyll a content. For Chl *a* analysis, samples (2 mL) harvested in late-exponential earlystationary phase and were centrifuged at 5000*g* for 5 min at 20°C. The supernatant was discarded and cell pellets stored frozen at -80°C until extraction and later analysis as previously

described in Baker et al. (2016). Samples were extracted in 3 mL volume of 3:2 90% acetone: 100% dimethyl sulfoxide extraction reagent in the dark at 4°C for 15 min (Shoaf and Lium 1976). Chlorophyll *a* was determined in a fluorometer (TD-700, Turner Designs, USA) using the non-acidification method of (Welschmeyer 1994). The fluorometer was calibrated with pure chlorophyll *a* (Sigma-Aldrich, USA), whose concentration was calculated from absorbance using the coefficients in Jeffrey et al. (1997).

Fatty acid (FA) composition. Given the fatty acid (FA) composition of membranes, has been shown to confer thermal sensitivity or tolerance in dinoflagellates (Tchernov et al. 2004), we examined the effect of temperature on saturated and unsaturated FA composition of CT- and HT-populations. Samples of 150 mL were harvested at late-exponential early- stationary phase and centrifuged at 5000g for 10 min at 20°C. The supernatant was discarded and the cell pellets were stored frozen at –20°C until analysis (within 6 months). Fatty-acid methyl ester (FAME) analysis was performed as per previously reported methods of Folch et al. (1957) and Carreau and Dubacq (1978). Lyophilised biomass in the tube was combined with a 3 mL mixture of chloroform and methanol 2:1 $\left[v/v \right]$ and vortexed for 3 min to allow lipids in algal cells to be extracted, the tube was then centrifuged at 2000g for 15 min. Supernatant was collected and the residue re-extracted twice with 2 mL of the above solvent mixture. Supernatants were pooled and evaporated to dryness under a stream of nitrogen. The resulting crude lipid mass was saponified in the presence of 1 mL 1% NaOH for 15 min at 55°C. Samples were allowed to cool, an internal standard was then added (10 μ L; nonadecanoic acid [1 mg \cdot mL⁻¹], Sigma Aldrich, NSW, Australia), followed by transesterification in the presence of 2 mL 5% methanolic HCl solution for 15 min at 55°C. To aid phase separation, 1 mL MilliQ was added, followed by 1 mL hexane. The reaction mixture was allowed to settle and the top, fatty acid enriched, non-polar phase was collected and transferred to a gas chromatography (GC) sample vial. Liquid-liquid extraction with hexane was repeated and the pooled hexane layer was evaporated to dryness under nitrogen. The resultant residue was reconstituted in 100 µL hexane and analysed by GC-MS (gas chromatography- mass spectrometry; Agilent 7890 series GC coupled to an Agilent

quadrupole MS (5975N) on a HP-5MS fused capillary column (5%-phenyl- methylpolysiloxan, 30 m long, 0.25 mm internal diameter, film thickness 0.25 μm, Agilent Technologies). Splitless mode of injection (5 μL volume) was used with a purge time of 1 min. Injection volume was 5 μL. The injector temperature was held at 280°C. Initial column temperature was 50°C (held for 2 min) and increased at a rate of 4°C · min⁻¹ to 220°C and then increased to 300°C at a rate of 60°C · min⁻¹ (held for 3 min). Data was analysed using Agilent GC Chemstation software where peaks were identified by matching the retention time and mass spectra of high purity FA (99.9%) standards (Sigma Aldrich, NSW, Australia). Acclimation and/or adaptation temperature is known to significantly influence the degree of FA saturation in membrane and storage lipids across a variety of ectotherms, including phytoplankton (Sushchik et al. 2003, Van Dooremalen et al. 2011). As a result, we calculated the unsaturation to saturation ratio (U/S ratio) as the ratio between the total proportion of all unsaturated fatty acids and the total proportion for all saturated fatty acids.

Thermal performance curves to examine thermal niche evolution

To examine trade-offs associated with adaptation to supra-optimal temperature, we quantified TPCs of functional traits (growth rate, electron transport rates, carbon assimilation, nitrate and phosphate uptake) and tested for differences in their thermal properties (V_{max} ; maximum trait value, T_{opt} ; thermal optimum of the trait, and the thermal niche width (the temperature range over which the trait value is positive, i.e., between the CT_{min} ; critical minimum temperature and CT_{max} ; critical maximum temperature) by fitting a thermal tolerance function to the data (Thomas et al. 2012) using the following equation:

$$f(T) = ae^{bT} \left[1 - \left(\frac{T - T_{av}}{(CT_{max} - CT_{min})/2} \right)^2 \right]$$

The shape of the TPC is controlled by three important temperature traits, CT_{min} and CT_{max} (which determine the thermal niche width), a and b (coeffecients of the 'Eppley' curve; Eppley 1972), an exponential relationship thought to provide the constraint on community-level phytoplankton growth as a function of temperature, and T_{av} which determines the location of the maximum quadratic portion of this function. When fitting curves to data for individual traits, it was found that estimates of CT_{min} produced unrealistic results and therefore it was necessary to constrain b and CT_{min} to positive values.

The point estimates for values of the thermal properties listed above were calculated as in Baker et al. (2016) using maximum likelihood estimates (MLE; assuming normally distributed errors) and the confidence intervals (CI) were calculated by parametric bootstrapping. To determine whether differences in thermal properties (i.e., maximum trait value, optimum temperature for trait and thermal niche width) for each trait were statistically significant between the CT- and HT-populations, we calculated the 95% CI for the difference between the two population means for each trait. We considered these differences to be significant at alpha = 0.05, if the 95% CI did not contain the null hypothesis (i.e., the mean difference was zero).

Reciprocal transplant assays to test for thermal adaptation of individual traits

To test for the specific adaptation of individual traits to supra-optimal temperatures we conducted a reciprocal transplant assay (Collins 2011) in which the HT- population was compared to the CT-population under their long-term growth conditions and vice-versa. An inoculum from the CT- and HT-populations was used to cultivate triplicate cultures of each population (250 mL) at control (25°C) and high-temperature (30°C) conditions, i.e., four treatments in total, under 100 μ mol photons \cdot m⁻² \cdot s⁻¹ (12 h:12 h, light:dark cycle). Following at least five generations of acclimation to 25°C and 30°C, we measured several functional traits

that influence competitive fitness, including growth rate, cell size, and photosynthetic traits such as saturation irradiance and maximum relative electron transport rates, and FA composition.

For all traits (growth rate, cell volume, unsaturation to saturation ratio (U/S ratio) of fatty acids, chlorophyll *a* content, ETR_{max} and E_k), data were first tested for normality and homogeneity of variance before performing a one-way analysis of variance (ANOVA) with subsequent Tukey's honestly significant differences (HSD) post-hoc comparisons. Differences were accepted as significant at p < 0.05. The hypothesis of a specific adaptation to supra-optimal temperature in the HT-population would be supported if mean trait values were not different (i.e., p > 0.05) between the CT- and HT-population at 30°C. Additionally, we used principle co- ordinates analysis (PCA) to visualise differences in FAME profiles between the CT- and HT-populations using the R version 1.1.423.

RESULTS

In this study, we observed a significant horizontal or vertical shift or both in the thermal niche for a number of key functional traits in HT populations of the tropical dinoflagellate, *Amphidinium massartii*. We were able to acquire and quantify the TPCs for these traits by measuring relative differences in trait performance (growth, carbon fixation, N and P uptake) between CT- and HT- populations in twelve temperature treatments across a large (~20°C) thermal range (including the selection environment of 30°C). We observed significant differences in the thermal properties (T_{opt} , CT_{min} , and CT_{max}) for multiple traits between the CTand HT- populations; meaning that the overall TPCs were significantly different. Overall, our results are consistent with the hypothesis that adaptation to supra-optimal temperature can result in a shift of the TPC and therefore a population's thermal niche.

Selection at high temperature (500 generations; 30°C) resulted in significant differences in the shape of the TPC relative to the control for several traits of *A. massartii*, including growth, gross primary productivity (GPP) and N and P uptake —identified by directional changes in important TPC parameters (Table 1; see Tables S1, S2 and S3 in the Supporting Information for statistical comparison of the bootstrapping results). Importantly, in comparison to the CT-population, fitted TPCs for growth revealed that the HT-population attained 20% greater maximum fitness $(V_{max} + 0.05 \cdot d^{-1})$ and ~3°C warmer T_{opt} (26.6°C; 95% CI, 26.0 to 28.2). In addition, a 40% contraction in the thermal niche width was evident, resulting from a warmer CT_{min} (+14.6°C; 95% CI, 5.1 to 15.5) and a cooler CT_{max} . Together, the simultaneous changes in CT_{min} , CT_{max} and T_{opt} resulted in a warm-shifted TPC (Fig. 1). It is noteworthy that although mortality was observed for both the CT- and HT- populations at temperatures \geq 38°C, the HT-population showed prolonged lethal exposure times (i.e., cells persisted for longer; Fig. 2)- demonstrating enhanced resistance to these extreme high temperatures. At 40°C, the lethal exposure time (i.e., the time at which 50% of the population was viable; Lex₅₀) was ~80 h longer for the HTpopulation compared to the CT-population at 40°C, with a Lex₅₀ of 160 h (R^2 =0.90), compared to 24 h in the CT-population (R^2 = 0.86; Fig. 2A). In contrast to the CT-population, where 50% of cells exposed to 38°C were not viable within 80 h (R² =0.96), the lethal exposure time for the HT-population could not be calculated but exceeded 200 h (Fig. 2B). Similar to growth, we observed an increase in the T_{opt} for N uptake in the HT-population, being \sim 1.63°C warmer than the CT-population, meaning maximum growth rates and maximum N acquisition occurred at warmer temperatures following long-term exposure to supra-optimal temperature. However, an increase in the *T*_{opt} was not observed across all traits; for example, there was no detectable change in the *T*_{opt} for GPP and P uptake in the HT-population (Table 1).

remaining traits was comparable between the CT- and HT-populations, with no relative change in niche widths observed for GPP, N and P uptake (Table 1).

Unlike the decreased niche width that was observed for growth, the thermal niche for

Living under long-term supra-optimal temperature also resulted in a vertical shift of the TPC. Specifically, we observed a consistent increase in the maximum trait value (V_{max} ; the trait value at the T_{opt}) across all measured traits (Table 1). The relative change in V_{max} was greatest for GPP, which increased by 75% (95% CI, 72 to 82%) in the HT-population compared to the CTpopulation, followed by P uptake (67%; 95% CI, 50 to 0%) and N uptake (43%; 95% CI, 29 to 89%). A vertical shift (or increased amplitude) in the TPCs for these traits suggests greater acquisition of dissolved C, N and P that occurred in HT cells when grown at optimal temperature conditions.

Complementing the TPC experiment which was used to examine the implications of adaptation on the thermal niches of important traits, we also conducted a reciprocal transplant assay to compare the phenotype expressed by HT-acclimated versus HT-adapted populations, and to ascertain whether the phytoplankton traits measured were plastic or evolvable following longterm exposure to high temperature. Under the selection temperature of 30°C, the mean values of overall fitness (growth rate), physiological (cellular chlorophyll concentration, maximum rETR_{max} and E_k) and morphological (cell size) traits were comparable between the CT and HT populations (CT30 versus HT30; Tukey's HSD; p> 0.05; Fig. 3).

In contrast to all other measured traits, we observed a strong and significant alteration in the lipid composition of HT-adapted cells that remained unchanged irrespective of assay temperature (Fig. 4). We used multivariate statistics in the form of principal coordinate analysis (PCA; Fig. 4) to compare the fatty acid profile between the CT- and HT-populations at 25 and 30°C by using values for each fatty acid (percentage of total fatty acids) which appeared in any of the samples (see Table S4 in the Supporting Information for fatty acid profile). Figure 4 indicates the separation of the CT25, CT30, HT25 and HT30 replicates on the first principal component (PC1). There was closer clustering of the CT25 and CT30 replicates and weaker

clustering of the HT25 and HT30 replicates. Separation between the CT- and HT-populations (CT25, CT30 versus HT25, HT30) was strongest on the PC1 that had the highest loading on EPA C20.5n3 (0.360), followed by arachidic acid C20.4.n6 (-0.344) and behenic acid C22.0 (-0.309) meaning it was these fatty acids that contributed towards most of the variability between the FAME profiles of the CT- and HT-populations. Overall, we see an increase in lipid saturation in the HT-population as evidenced by the decrease in the U/S ratio compared to the CT- population, irrespective of assay temperature (CT30 versus HT30; Tukey's HSD; p= 0.022; Fig. 3C).

Reversibility of HT adaptation was not consistent across all measured functional traits. Some traits remained fixed and did not revert during a short re-acclimation period (5 generations) to the control temperature (i.e., HT30 versus HT25 population; Tukey's HSD; p> 0.05) including the U/S ratio of lipids (Fig. 3C) and ETR_{max} (Fig. 3E). However, the increased pigmentation of cells at high temperature was dynamically altered to levels expressed by the CT-population and is therefore reversible (i.e., HT30 versus CT25 population; Fig. 3D). Other functional traits of the high-temperature population changed in response to their re-acclimation to control temperatures but did not have the same values as the CT population. For example, cell volume in the HT-population decreased by 60% when grown at 25°C (HT25) compared to 30°C (HT30), but still remained 50% smaller than the CT-population (i.e., HT25 versus CT25; Tukey's HSD; p < 0.001; Fig. 3B). The E_k of the HT-population increased six-fold when grown at 25°C compared to 30°C (HT25 vs. HT30; Tukey's HSD p <0.001; Fig. 3F), with HT30 similar to the CT population. Consequently, some traits of the phenotype remained fixed (e.g., FA composition) while others were dynamic but did not necessarily reflect values of the CT-population (e.g., smaller cell size). Therefore, reversibility of FT in the HT-population appears to be trait-specific, with only cell Chlorophyll *a* quota being fully reversible.

In summary, the overall phenotype of the HT-population was a combination of both fixed and reversible traits as evidenced by comparisons between the CT- and HT-populations at the CT (25°C; 5 generations). The biochemical composition of FA remained similar in the HT-population when re-exposed to 25°C for several generations (Fig. 3C), whereas other cellular characteristics were dynamic (e.g., chlorophyll *a* content; Fig. 3D). These results demonstrate the time-scale of thermal exposure is important, especially when conducting multi-trait assessments, because some cellular changes may take longer to adjust than others, for example, weeks compared to hours or days.

DISCUSSION

For the first time in a dinoflagellate, we examined the long-term response of individual functional traits to supra-optimal temperature. We have shown that through shifting its TPC, an organism can alter the thermal properties of key traits; effectively changing their physiological limits to more closely suit their new environment. In the context of global warming, this evolution of trait TPCs may provide an additional mechanism to supplement standing genetic and phenotypic diversity which allows the persistence of existing species (Collins and Gardner 2009).

Consistent with previous studies of high temperature adaptation (bacteriophages, Knies et al. 2006; coccolithophores, Listmann et al. 2016), we observed a horizontal shift in the TPC for growth, centered at a warmer T_{opt} as well as enhanced thermal resistance at extreme high temperatures. These results suggest that adaptation has the capacity to alter the current physiological limits of species and to some extent, track the expected increase in average SST across the global ocean (Boyd et al. 2014). This suggests that tropical phytoplankton may not be

as vulnerable to ocean warming as previously thought (Thomas et al. 2012). Indeed, in other model species such as fruit flies (*Drosophila*), predicted organism resilience to climate change is enhanced when evolutionary processes are incorporated into species distribution models (Bush et al. 2016). Consequently, models that use TPC properties (e.g., the T_{opt}) to forecast changes in phytoplankton distribution (Thomas et al. 2012) and ocean productivity (Taucher and Oschlies 2011), should consider the adaptive capacity of these key parameters to increase the accuracy of future projections.

Trade-offs during thermal adaptation can influence the evolution of the TPC, altering its shape and position (Huey and Kingsolver 1989, Angilletta et al. 2003, Knies et al. 2006). Here, we found evidence of a generalist-specialist trade-off, whereby the TPC of the HT population of *Amphidinium massartii* displayed enhanced performance within a narrower range of intermediate temperatures and a decrease in performance at other temperatures (Fig. 1). Hightemperature-specialization may equip this tropical microbial eukaryote with an advantageous life strategy to 'bloom' during the hotter summer months or survive the warmer average SST predicted in the future ocean (IPCC 2014). Furthermore, we observed longer lethal exposure times in HT populations of *A. massartii* (≥38°C; see Fig. 2B). These results suggest that additional benefits of a generalist-specialist trade-off may enable this organism's persistence (rather than reproduction) during short-lived hostile periods (Pörtner 2002), that are predicted to become more frequent but also potentially more irregular with climate change (Meehl and Tebaldi 2004).

Although high-temperature-specialization may prove beneficial for microbial phototrophs living in generally warmer oceans (increase in average SST) exposed to more frequent 'heat waves', our results also suggest costs associated with a generalist-specialist trade-off. Most notably, we observed higher maximum uptake rates of C, N and P in the HT-population, which we interpret

as facilitating the higher maximum growth rates at intermediate temperatures. However, by fine-tuning these traits for enhanced performance at higher temperature, HT populations may only be successful when nutrients are readily available, for example, in coastal environments supported by nutrient-rich run-off. Therefore, living at supra-optimal temperature has not only redefined *A. massartii's* thermal niche, but also its nutrient-niche. These data show that the trade-offs in underlying traits that occur to support changes in growth along one environmental gradient may alter their competiveness along one or more other environmental gradients (Litchman et al. 2012).

The reciprocal transplant assay revealed that the overall phenotype of the HT-population was a combination of both fixed and reversible traits. Whilst some cellular characteristics were dynamic (e.g., chlorophyll *a* content), the FA composition of the HT-population remained tuned to their long-term culturing conditions at HT, irrespective of assay temperature. Alterations in specific FA such as the relative decrease in EPA, and increases in arachidic acid and behrenic acid changed in accordance with previous observations of short-term exposures to high-temperature (Bigogno et al. 2002, Rousch et al. 2003, Lei et al. 2012). However, the overall increase in FA saturation (decrease in U/S ratio) appears characteristic of the HT-population and may be an important mechanism for adaptation to high temperature. For example, saturated FA are less easily oxidized by oxygen radicals and may offer protection to membranes from attack by reactive oxygen species (Lesser 2006).

Consequently, the results from the reciprocal transfer assay suggest that all phytoplankton traits may not respond similarly to supra-optimal temperature. The temperature-induced shift of some traits suggests that they may be more important than other traits in determining the overall fitness of the resultant phenotype. Specifically, for the marine microbial phototroph in this study, it appears that a biochemical adaptation (rather than a physiological or

morphological adaptation) may be an underlying mechanism that alters the thermal niche in HT populations of *Amphidinium massartii*.

The data presented here are central to describing and understanding the physiological and evolutionary responses to temperature change among phytoplankton (Reusch and Boyd 2013), and are consistent with evolutionary experiments performed on the coccolithophore Emiliania *huxleyii* and the green alga *Chlamydomonas reinhardtii*, where *T*_{opt} also shifted upwards (Listmann et al. 2016, Schaum et al. 2017). However, it is noteworthy that while the present study measured an evolutionary response to warming (revealed by switching the HT population to the CT condition and showing an irreversible fatty acid saturation), only one population per treatment was used (n = 1), which limits our ability to attribute the results to long-term temperature exposure, as populations may diverge in performance over the long-term. Furthermore, because the founding inoculum for the selection line was not re-isolated from a single cell, it is likely that the culture contained a significant amount of genetic variation due to its relatively large population size (between 2.5×10^5 and 2.5×10^7 cells \cdot mL⁻¹) and time spent in culture (> 25 y) before selection was imposed. Therefore, our observation of a generalistspecialist trade-off for Amphidinium massartii is potentially one of numerous evolutionary outcomes to living at supra-optimal temperature but nevertheless shows the potential within a single genotype of a species to rapidly (<500 generations) adapt. For example, while Listmann et al. (2016) report an increase in the CT_{max} with long-term warming in a temperate species of coccolithophore, we report an increase in the CT_{min} for a tropical dinoflagellate. These differences highlight that the mechanisms underlying the different modes of TPC evolution remain unknown and should be further investigated in future long-term experiments. To achieve a more in-depth understanding of how adaptation to warming SST affects the thermal sensitivities of phytoplankton, similar experiments to those presented here should be conducted for other phytoplankton functional groups and with a greater number of

independent populations per treatment. This data will be vital for predicting the direction and magnitude of change in species distributions as well as future ocean primary production and biogeochemical cycling.

AUTHOR CONTRIBUTIONS

KB, MD and PR conceived and designed the experiment. KB, DR, UK and MD acquired the data. KB, DR and CE analyzed the data. KB, CE, PR and MD interpreted the data. KB drafted the work and all authors critically revised the work for intellectual content. All authors approved the final version to be published and agreed to be accountable for all aspects of the work.

ACKNOWLEDGMENTS

The authors would like to thank Professor Madeleine van Oppen and Dr. Antonio Flores-Moya for their initial discussions that led to the foundations of the thermal adaptation work, Lis Hou for initially establishing the laboratory cultures used for this experiment and Professor Maria Byrne for access to the thermal gradient blocks. KB would like to thank Dr. Karine Leblanc, Dr. Michael Lomas and Professor Philip Boyd for their thoughtful critique on her 2016 Ph.D dissertation at the University of Techonology Sydney, of which this investigation was a part. This research was funded by a student scholarship to KB awarded through the School of Life Sciences and Climate Change Cluster (C3), University of Technology Sydney and an Australian Research Council Discovery Project (DP14010134) to MD. The authors declare that the research was conducted in the absence of any commercial or financial relationships that could be construed as a potential conflict of interest.

REFERENCES

- Angilletta Jr, M. J. 2013. Biochemical and Physiological Adaptations. *The Princeton Guide to Evolution.* pp. 282.
- Angilletta Jr, M. J., Wilson, R. S., Navas, C. A. & James, R. S. 2003. Tradeoffs and the evolution of thermal reaction norms. *Trends Ecol. Evol.* 18:234-40.
- Baker, K. G., Robinson, C. M., Radford, D. T., McInnes, A. S., Evenhuis, C. & Doblin, M. A. 2016.
 Thermal performance curves of functional traits aid understanding of thermally induced changes in diatom-mediated biogeochemical fluxes. *Front. Mar. Sci.* 3:44.
- Behrenfeld, M. J., O'Malley, R. T., Siegel, D. A., McClain, C. R., Sarmiento, J. L., Feldman, G. C., Milligan, A. J., Falkowski, P. G., Letelier, R. M. & Boss, E. S. 2006. Climate-driven trends in contemporary ocean productivity. *Nature* 444:752-55.
- Bennett, A. F. & Lenski, R. E. 2007. An experimental test of evolutionary trade-offs during temperature adaptation. *Proc. Natl. Acad. Sci. USA* 104:8649-54.
- Bigogno, C., Khozin-Goldberg, I., Adlerstein, D. & Cohen, Z. 2002. Biosynthesis of arachidonic acid in the oleaginous microalga Parietochloris incisa (Chlorophyceae): radiolabeling studies. *Lipids* 37:209-16.
- Boyd, P. W., Strzepek, R., Fu, F. & Hutchins, D. A. 2010. Environmental control of open-ocean phytoplankton groups: Now and in the future. *Limnol. Oceanogr.* 55:1353-76.

Bush, A., Mokany, K., Catullo, R., Hoffmann, A., Kellermann, V., Sgrò, C., McEvey, S. & Ferrier, S. This article is protected by copyright. All rights reserved. 2016. Incorporating evolutionary adaptation in species distribution modelling reduces projected vulnerability to climate change. *Ecol. Lett.* 19:1468-78.

- Carreau, J. P. & Dubacq, J. P. 1978. Adaptation of a macro-scale method to the micro-scale for fatty acid methyl transesterification of biological lipid extracts. *J. Chromatogr.* 151:384-90.
- Claquin, P., Probert, I., Lefebvre, S. & Veron, B. 2008. Effects of temperature on photosynthetic parameters and TEP production in eight species of marine microalgae. *Aquat. Microb. Ecol.* 51:1-11.
- Collins, S. 2011. Many possible worlds: expanding the ecological scenarios in experimental evolution. *Evol. Biol* 38:3-14.
- Collins, S. & Bell, G. 2004. Phenotypic consequences of 1,000 generations of selection at elevated CO2 in a green alga. *Nature* 431:566-69.
- Collins, S. & Gardner, A. 2009. Integrating physiological, ecological and evolutionary change: a Price equation approach. *Ecol. Lett.* 12:744-57.
- Collins, S., Rost, B. & Rynearson, T. A. 2014. Evolutionary potential of marine phytoplankton under ocean acidification. *Evol. App.* 7:140-55.
- Davison, I. R. 1991. Environmental effects on algal photosynthesis: temperature. *J. Phycol.* 27:2-8.
- Elena, S. F. & Lenski, R. E. 2003. Evolution experiments with microorganisms: the dynamics and genetic bases of adaptation. *Nat. Rev. Genet.* 4:457-69.
- Eppley, R. W. 1972. Temperature and phytoplankton growth in the sea. *Fish. Bull.* 70:1063-85.
- Falkowski, P. G., Barber, R. T. & Smetacek, V. 1998. Biogeochemical controls and feedbacks on ocean primary production. *Science* 281:200-06.

- Feng, Y., Warner, M. E., Zhang, Y., Sun, J., Fu, F. X., Rose, J. M. & Hutchins, D. A. 2008. Interactive effects of increased pCO2, temperature and irradiance on the marine coccolithophore Emiliania huxleyi (Prymnesiophyceae). *Eur. J. Phycol.* 43:87-98.
- Flynn, K. J. 2001. A mechanistic model for describing dynamic multi-nutrient, light, temperature interactions in phytoplankton. *J. Plankton Res.* 23:977-97.
- Folch, J., Lees, M. & Sloane-Stanley, G. H. 1957. A simple method for the isolation and purification of total lipids from animal tissues. *J. Biol. Chem.* 226:497-509.
- Fu, F. X., Zhang, Y., Warner, M. E., Feng, Y., Sun, J. & Hutchins, D. A. 2008. A comparison of future increased CO₂ and temperature effects on sympatric *Heterosigma akashiwo* and *Prorocentrum minimum. Harmful Algae* 7:76-90.
- Geider, R. J., MacIntyre, H. L. & Kana, T. M. 1997. Dynamic model of phytoplankton growth and acclimation: responses of the balanced growth rate and the chlorophyll a: carbon ratio to light, nutrient-limitation and temperature. *Mar. Ecol. Prog. Ser.* 148:187-200.
- Guillard, R. R. & Ryther, J. H. 1962. Studies of marine planktonic diatoms. I. *Cyclothella nana* Hustedt and *Detonula confervacea* Gran. *Can. J. Microbiol./Rev. Can. Microbiol.* 8:229-39.
- Hillebrand, H., Dürselen, C. D., Kirschtel, D., Pollingher, U. & Zohary, T. 1999. Biovolume calculation for pelagic and benthic microalgae. *J. Phycol.* 35:403-24.
- Hoenig, M., Lee, R. J. & Ferguson, D. C. 1989. A microtiter plate assay for inorganic phosphate. *J. Biochem. Biophys. Methods* 19:249-51.
- Hoffmann, A. A. & Sgro, C. M. 2011. Climate change and evolutionary adaptation. *Nature* 470:479-85.
- Hou, L. 2011. *Variability in the thermal response of the microalga* Amphidinium massartii. PhD Thesis, University of Technology Sydney, Sidney, Australia, 69 pp.

- differently: evidence through a mechanistic approach. Proc. R. Soc. B 278:3534-43.
 Huey, R. B. & Kingsolver, J. G. 1989. Evolution of thermal sensitivity of ectotherm performance. Trends Ecol. Evol. 4:131-35.
 Huey, R. B. & Stevenson, R. 1979. Integrating thermal physiology and ecology of ectotherms: a discussion of approaches. Am. Zool. 19:357-66.
 IPCC 2014. Climate Change 2014: Synthesis Report. Contribution of Working Groups I, II and III to the Fifth Assessment Report of the Intergovernmental Panel on Climate Change, 169 pp.
 Jassby, A. D. & Platt, T. 1976. Mathematical formulation of the relationship between photosynthesis and light for phytoplankton. Limnol. Oceanogr. 21:540-47.
 Johnston, I. A. & Bennett, A. F. 1996. Animals and Temperature: Phenotypic and Evolutionary Adaptation. Cambridge University Press, Cambridge, UK, 436 pp.
 Knies, J. L., Izem, R., Supler, K. L., Kingsolver, J. G. & Burch, C. L. 2006. The genetic basis of
 - Knies, J. L., Izem, R., Supler, K. L., Kingsolver, J. G. & Burch, C. L. 2006. The genetic basis of thermal reaction norm evolution in lab and natural phage populations. *PLoS Biol.* 4:e201.

Huertas, I. E., Rouco, M., López-Rodas, V. & Costas, E. 2011. Warming will affect phytoplankton

- Kulk, G., de Vries, P., van de Poll, W. H., Visser, R. J. W. & Buma, A. G. J. 2012. Temperaturedependent growth and photophysiology of prokaryotic and eukaryotic oceanic picophytoplankton. *Mar. Ecol. Prog. Ser.* 466:43–55.
- LaJeunesse, T. C., Lambert, G., Andersen, R. A., Coffroth, M. A. & Galbraith, D. W. 2005. Symbiodinium (Pyrrhophyta) genome sizes (DNA content) are the smallest among dinoflagellates. J. Phycol. 41:880-86.
- Lee, J. J., Olea, R., Cevasco, M., Pochon, X., Correia, M., Shpigel, M. & Pawlowski, J. 2003. A marine dinoflagellate, *Amphidinium eilatiensis* n. sp., from the benthos of a mariculture sedimentation pond in Eilat, Israel. *J. Eukaryot. Microbiol.* 50:439-48.

- Lei, A., Chen, H., Shen, G., Hu, Z., Chen, L. & Wang, J. 2012. Expression of fatty acid synthesis genes and fatty acid accumulation in Haematococcus pluvialis under different stressors. *Biotechnol. Biofuels* 5:18.
- Lenski, R. E. & Bennett, A. F. 1993. Evolutionary response of *Escherichia coli* to thermal stress. *Am. Nat.*:S47-S64.
- Lesser, M. P. 2006. Oxidative stress in marine environments: biochemistry and physiological ecology. *Annu. Rev. Physiol.*, 68:253-78.
- Listmann, L., LeRoch, M., Schlüter, L., Thomas, M. K. & Reusch, T. B. H. 2016. Swift thermal reaction norm evolution in a key marine phytoplankton species. *Evol. App.* 24:2239-61.
- Litchman, E., Edwards, K. F., Klausmeier, C. A. & Thomas, M. K. 2012. Phytoplankton niches, traits and eco-evolutionary responses to global environmental change. *Mar. Ecol. Prog. Ser.* 470:235-48.
- Litchman, E. & Klausmeier, C. A. 2008. Trait-based community ecology of phytoplankton. *Annu. Rev. Ecol., Evol. Syst.* 39:615-39.
- Lohuis, M. R. & Miller, D. J. 1998. Genetic transformation of dinoflagellates (*Amphidinium* and *Symbiodinium*): expression of GUS in microalgae using heterologous promoter constructs. *Plant J.* 13:427-35.
- Meehl, G. A. & Tebaldi, C. 2004. More intense, more frequent, and longer lasting heat waves in the 21st century. *Science* 305:994-97.
- Pörtner, H. O. 2002. Climate variations and the physiological basis of temperature dependent biogeography: systemic to molecular hierarchy of thermal tolerance in animals. *Comp. Biochem. Physiol., A: Mol. Integr. Physiol.* 132:739-61.
- Ralph, P. J. & Gademann, R. 2005. Rapid light curves: a powerful tool to assess photosynthetic activity. *Aquat. Bot.* 82:222-37.

Raven, J. A. & Geider, R. J. 1988. Temperature and algal growth. *New Phytol*.:441-61.

- Reboud, X., Majerus, N., Gasquez, J. & Powles, S. 2007. *Chlamydomonas reinhardtii* as a model system for pro - active herbicide resistance evolution research. *Biol. J. Linn. Soc.* 91:257-66.
- Reusch, T. B. & Boyd, P. W. 2013. Experimental evolution meets marine phytoplankton. *Evolution* 67:1849-59.
- Robison, J. D. & Warner, M. E. 2006. Differential impacts of photoacclimation and thermal stress on the photobiology of four different phylotypes of *Symbiodinium* (Pyrrhophyta). *J. Phycol.* 42:568-79.
- Rousch, J. M., Bingham, S. E. & Sommerfeld, M. R. 2003. Changes in fatty acid profiles of thermointolerant and thermo-tolerant marine diatoms during temperature stress. *J. Exp. Mar. Biol. Ecol.* 295:145-56.
- Schaum, C. E., Barton, S., Bestion, E., Buckling, A., Garcia-Carreras, B., Lopez, P., Lowe, C., Pawar,
 S., Smirnoff, N. & Trimmer, M. 2017. Adaptation of phytoplankton to a decade of
 experimental warming linked to increased photosynthesis. *Nat. Ecol. Evol.* 1:0094.
- Schluter, L., Lohbeck, K. T., Gutowska, M. A., Groger, J. P., Riebesell, U. & Reusch, T. B. H. 2014.
 Adaptation of a globally important coccolithophore to ocean warming and acidification.
 Nat. Clim. Cha. 4:1024–30.
- Schnetger, B. & Lehners, C. 2014. Determination of nitrate plus nitrite in small volume marine water samples using vanadium (III) chloride as a reduction agent. *Mar. Chem.* 160:91-98.
- Suggett, D. J., Goyen, S., Evenhuis, C., Szabó, M., Pettay, D. T., Warner, M. E. & Ralph, P. J. 2015.
 Functional diversity of photobiological traits within the genus Symbiodinium appears to be governed by the interaction of cell size with cladal designation. *New Phytol.* 208:

- Sushchik, N. N., Kalacheva, G. S., Zhila, N. O., Gladyshev, M. I. & Volova, T. G. 2003. A temperature dependence of the intra-and extracellular fatty-acid composition of green algae and cyanobacterium. *Russ. J. Plant Physl.* 50:374-80.
 - Taucher, J. & Oschlies, A. 2011. Can we predict the direction of marine primary production change under global warming? *Geophys. Res. Lett.* 38:L02603.
 - Tchernov, D., Gorbunov, M. Y., de Vargas, C., Narayan Yadav, S., Milligan, A. J., Häggblom, M. & Falkowski, P. G. 2004. Membrane lipids of symbiotic algae are diagnostic of sensitivity to thermal bleaching in corals. *Proc. Natl. Acad. Sci. USA* 101:13531-35.
 - Thomas, M. K., Kremer, C. T., Klausmeier, C. A. & Litchman, E. 2012. A global pattern of thermal adaptation in marine phytoplankton. *Science* 338:1085-88.
 - Van Dooremalen, C., Koekkoek, J. & Ellers, J. 2011. Temperature-induced plasticity in membrane and storage lipid composition: thermal reaction norms across five different temperatures. *J. Insect Physiol.* 57:285-91.
 - Zhu, L., Bloomfield, K. J., Hocart, C. H., Egerton, J. J. G., O'Sullivan, O. S., Penillard, A., Weerasinghe,
 L. K. & Atkin, O. K. 2018. Plasticity of photosynthetic heat tolerance in plants adapted to
 thermally contrasting biomes. *Plant, Cell Environ.* 41:1251-62.

TABLES

Table 1. Shift in the thermal properties (thermal optimum T_{opt} ; trait value at thermal optimum V_{max} ; niche width; critical maximum temperature CT_{max} ; and critical minimum temperature CT_{min}) of *Amphidinium massartii* following 500 generations of adaptation to supra-optimal temperature (30°C) for functional traits measured. Changes were calculated as the relative difference in estimated parameters (based on non-linear curve fits and parameteric bootstrapping) between the CT and HT population. Differences were considered to be significant at alpha = 0.05, if the 95% confidence internals did not contain zero (i.e., mean difference was not zero) and are indicated by asterisks. Values in brackets are the 95% confidence intervals.

				Thermal Property		
		T_{opt} (°C)	V _{max} (%)	Niche width (°C)	<i>CT_{max}</i> (°C)	CT _{min} (°C)
	Growth Rate	+2.83*	+20.56*	-15.88*	-1.48*	+14.60*
		[0.55 , 5.54]	[17.36, 23.96]	[-17.71 , -6.72]	[-2.69 , -0.48]	[5.06 , 15.55]
	Gross primary productivity	+0.81	+75.81*	-2.58	+0.10	+1.98
	Gross primary productivity	[-7.57, 4.62]	[9.91, 133.41]	[-17.29 , 10.99]	[-2.21 , 2.17]	[-19.02 , 17.62]
	N uptake	+1.63*	+43.64*	-1.43	-0.79	+0.23
	-	[0.03 , 3.07]	[-38.06, 136.24]	[-10.09 , 3.71]	[-2.23 , 0.37]	[-4.82 , 9.60]
	P uptake	+1.36	+52.92*	-1.83	-1.54*	+0.02
	r	[-0.10 , 2.69]	[48.42, 58.32]	[-10.34, 1.29]	[-2.73,-0.36]	[-2.93, 9.00]

Table S1. Estimated thermal performance curve (TPC) parameters and associated uncertainty for control-temperature (CT)- and high-temperature (HT)-populations calculated from parametric bootstrapping for growth rate and gross primary productivity fitted using Equation 5.4; thermal optimum T_{opt} , trait value at thermal optimum V_{max} , critical maximum temperature CT_{max} , critical minimum temperature CT_{min} and thermal niche width. The mean squared error (MSE) approximation provides a measure of uncertainty of the fitted function, whereas the 95% confidence intervals (CI) provide a measure of uncertainty on the derived parameters. The shift in TPC associated with HT adaptation (Δ HT) was calculated as the difference in derived parameters between the CT and HT population. These differences were considered to be significant at alpha = 0.05, if the 95% CI did not contain 0 (i.e. the null hypothesis rejected) and are indicated as bold text.

Table S2. Estimated thermal performance curve (TPC) parameters and associated uncertainty for control-temperature (CT)- and high-temperature (HT)-populations calculated from parametric bootstrapping for non-photochemical quenching (NPQ) and effective quantum yield (ϕ_{PSII}) fitted using Equation 5.4; thermal optimum T_{opt} , trait value at thermal optimum V_{max} , critical maximum temperature CT_{max} , critical minimum temperature CT_{min} and thermal niche width. The mean squared error (MSE) approximation provides a measure of uncertainty of the fitted function, whereas the 95% confidence intervals (CI) provide a measure of uncertainty on the derived parameters. The shift in TPC associated with HT adaptation (Δ HT) was calculated as the difference in derived parameters between the CT and HT population. These differences were considered to be significant at alpha = 0.05, if the 95% CI did not contain 0 (i.e., the null hypothesis rejected) and are indicated as bold text.

FA).

Table S3. Estimated thermal performance curve (TPC) parameters and associated uncertainty for control-temperature (CT)- and high-temperature (HT)-populations calculated from parametric bootstrapping for nitrate (NO_x) and phosphate (PO₄) uptake fitted using Equation 5.4; thermal optimum T_{opt} , trait value at thermal optimum V_{max} , critical maximum temperature CT_{max} , critical minimum temperature CT_{min} and thermal niche width. The mean squared error (MSE) approximation provides a measure of uncertainty of the fitted function, whereas the 95% confidence intervals (CI) provide a measure of uncertainty on the derived parameters. The shift in TPC associated with HT adaptation (Δ HT) was calculated as the difference in derived parameters between the CT and HT population. These differences were considered to be significant at alpha = 0.05, if the 95% CI did not contain 0 (i.e., the null hypothesis rejected) and are indicated as bold text.

Table S4. Modifications in fatty acid composition in percentage of total fatty acid methyl esters (FAME) of the tropical dinoflagellate *Amphidinium massartii* following three y (~500 generations) of exposure to control (CT) or +5°C (HT) conditions (25°C versus 30°C). Values are the mean percentage of total fatty acid (± standard error of the mean, n = 3 for each group). ME is methyl ester, Σ SAFA indicates the sum of all fatty acids (FA) with no double bonds (i.e., saturated FA), Σ MUFA indicates the sum of all FA with one double bond (i.e., polyunsaturated FA).

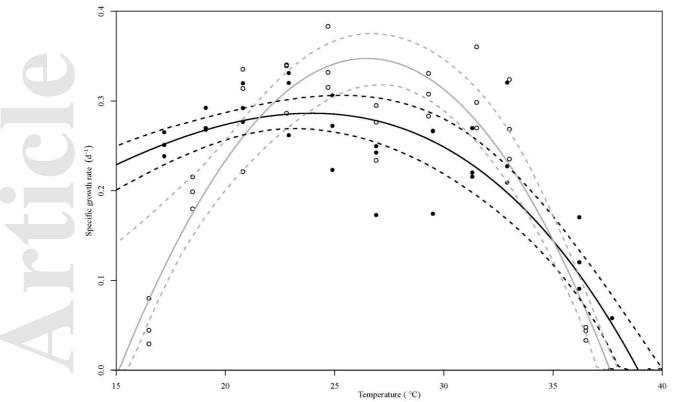
Figure 1. Thermal performance curves (TPC) of fitness in the dinoflagellate *Amphidinium massartii*. Growth rate is depicting as a function of temperature in the control-temperature (CT)-population (closed symbols; n = 36, MSE = 0.0022) and high-temperature (HT)-population (open symbols; n = 36, MSE = 0.0017). Each symbol represents a distinct biological replicate. Solid lines represent maximum likelihood estimates (MLE) and broken lines correspond to the 95% confidence intervals (CI) of the bell-shaped function (Equation 5.4), of the CT and HT-populations (black and grey lines, respectively). See Table S1 for statistical comparison of the bootstrapping results.

Figure 2. Exposure-response curves in the dinoflagellate *Amphidinium massartii*. Figure represents the percentage of viable cells (negative for SYTOX green nucleic acid stain) as a function of time (hours) of control-temperature (CT)-population closed symbols; n = 36) and high-temperature (HT)-populations (open symbols; n = 36) assayed at the two highest temperatures (A) 40°C and (B) 38°C where growth was not observed. Each symbol represents a distinct biological replicate. Solid lines represent maximum likelihood estimates (MLE) of the exposure-response function of each population.

Figure 3. Physiological characterization of the tropical dinoflagellate *Amphidinium massartii* following three y (~500 generations) of exposure to control (CT) or +5°C (HT) conditions (25°C versus 30°C). Mean trait values (± standard error of the mean, n = 3 for each group) of control-temperature (CT)-population and high-temperature (HT)populations when assayed at control (25°C) and high (30°C) temperatures (blue versus red bars, respectively) of (A) growth, (B) cell volume, (C) U/S ratio (unsaturated:saturated fatty acids), (D) chlorophyll *a* content per cell volume, (E)

maximum electron transport rate, and (F) saturating irradiance. Letters above bars represent Tukey's honestly significant difference (HSD) between groups (p < 0.05).

Figure 4. Principle components analysis (PCA) of samples from of the tropical dinoflagellate *Amphidinium massartii* following three y (~500 generations) of exposure to control (CT) or +5°C (HT) conditions (25°C versus 30°C). The first two axes of the PCA are represented with principle coordinate axis 1 (PC1; 54.9% variability) and principle coordinate axis 2 (PC2; 18.1% variability). Each label represents a distinct biological replicate (i.e., sample); n=3 for each treatment group, except CT25 (n=2; one sample was lost during analysis).



Accepted

